C. R. Physique 17 (2016) 455–470

Contents lists available at ScienceDirect

Comptes Rendus Physique

www.sciencedirect.com

Condensed matter physics in the 21st century: The legacy of Jacques Friedel

Quantum kagome frustrated antiferromagnets: One route to quantum spin liquids

Frustration dans les composés antiferromagnétiques quantiques sur réseau kagomé : une voie vers les liquides de spin

Philippe Mendels *, Fabrice Bert

Laboratoire de physique des solides, CNRS, Université Paris-Sud, Université Paris-Saclay, 91405 Orsay cedex, France

ARTICLE INFO

Article history:
Available online 21 December 2015

Keywords:
Quantum antiferromagnetism
Kagome
Spin liquid

Mots-clés :
Antiferromagnétisme quantique
Kagome
Liquide de spin

ABSTRACT

After introducing the field of Highly Frustrated Magnetism through the quest for a quantum spin liquid in dimension higher than one, we focus on the emblematic case of the kagome network. From a theoretical point of view, the simple Heisenberg case for an antiferromagnetic kagome lattice decorated with quantum spins has been a long-standing problem, not solved yet. Experimental realizations have remained scarce for long until the discovery of herbertsmithite $ZnCu_3(OH)_6Cl_2$ in 2005. This is one of the very few quantum kagome spin liquid candidates that triggered a burst of activity both on theory and experiment sides. We give a survey of theory outcomes on the "kagome" problem, review the experimental properties of that model candidate and shortly discuss them with respect to recent theoretical results.

RÉSUMÉ

Après avoir introduit la thématique du magnétisme fortement frustré par le biais de la recherche d'un état liquide de spin quantique au-delà de la dimension 1, nous discutons en détail le cas emblématique du réseau kagome. D'un point de vue théorique, le cas le plus simple de l'hamiltonien d'Heisenberg sur une telle géométrie décorée de spins quantiques en interaction antiferromagnétique est un problème ancien, non encore résolu. Les réalisations expérimentales sont restées rares jusqu'à la découverte de l'herbertsmithite $ZnCu_3(OH)_6Cl_2$ en 2005. C'est l'une des seules réalisations expérimentales d'un liquide de spin quantique sur réseau kagome dont la découverte a engendré une intense activité à la fois théorique et expérimentale. Nous donnons un aperçu des résultats théoriques sur ce problème kagome, passons en revue les propriétés expérimentales de ce composé « modèle » et les discutons dans le cadre des résultats théoriques les plus récents.

* Corresponding author.
E-mail address: mendels@lps.u-psud.fr (P. Mendels).

http://dx.doi.org/10.1016/j.crhy.2015.12.001

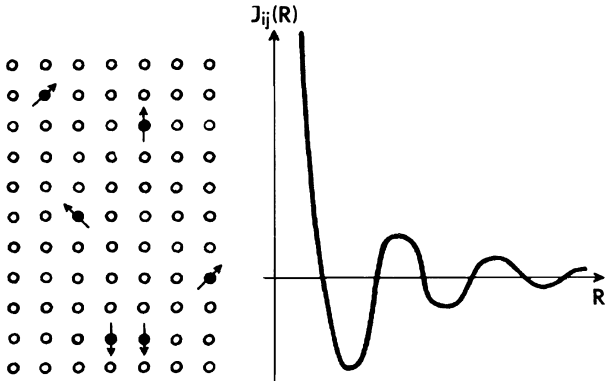

Fig. 1. From Ref. [2]: sketch of magnetic moments randomly diluted in a metallic matrix, and the resulting RKKY exchange integral plotted as a function of distance.

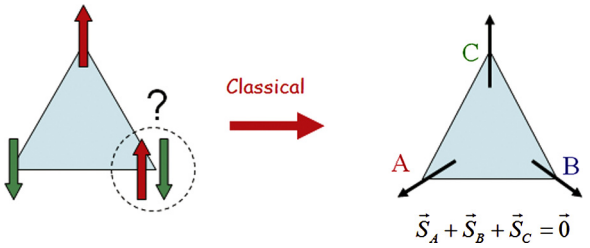

Fig. 2. Left: frustration on a triangular lattice. Right: classical minimization of the interaction energy. One of the two possible chiralities, defined as $(\vec{S}_A, \vec{S}_B, \vec{S}_C)$, is represented here.

1. Introduction

1.1. From disorder-induced to geometric frustration

Broken symmetries are ubiquitous at all scales in physics from high-energy to condensed-matter physics. The transition from para- to ferro- or antiferro-magnetism is one of the common textbook examples: breaking the rotational invariance occurs through a selection of a specific direction of the magnetization at a transition temperature of the order of the energy of interactions between moments. This characteristic temperature named Curie (ferro case) or Néel (antiferro case) temperature is commonly derived from a high-temperature mean-field treatment of the magnetic Hamiltonian.

The transition from liquids to crystalline solids is another example. In contrast, from a structural aspect, glasses constitute a remarkable exception where atoms do not order in a periodic lattice. Tracing it back to the field of magnetism, randomness typical of glasses can be generated by dissolving transition metal magnetic impurities in a metallic matrix, e.g., CuMn. Friedel-like oscillations of the host spin polarization around impurities indeed give birth to a random effective interaction between impurity moments, oscillating and decreasing with distance. This generates a quenched disordered magnet named RKKY spin glass [1] (Fig. 1). Randomness is responsible for frustration, a concept thus named to coin the impossibility to minimize pair-wise interactions [3]. Disorder and frustration – here resulting itself from disorder – were identified as the two ingredients presiding over the formation of a spin glass.

Actually, frustration, although not thus named initially, was already present in many well-known disorder-free cases; helimagnets and Ising's model on the triangular lattice are two such examples on the experimental and theoretical sides. On such regular lattices, the magnetic structure results from an energy compromise dictated by frustration (Fig. 2).

At variance with this paradigm, P.W. Anderson, in his 1973 famous resonating valence bond state (RVB) conjecture proposed that in a triangular-based antiferromagnetic lattice, frustration conspires with quantum fluctuations maximized for spins $S = 1/2$, to destabilize conventional Néel states [4] – note that this was before spin glass and the name of frustration came out. Such an RVB intricate state is made of all possible disordered pavings with singlet dimers of neighboring spins (Fig. 3). This therefore prevents from any symmetry breaking at $T = 0$ and is in stark contrast with the ordered states of conventional magnets.

Energetic classical arguments comparing classical Néel ordered states and dimer singlet configurations shown in Fig. 4 clearly explain why in the 1D case, dimers can be stabilized, why it was an open question for the triangular lattice – it is now clear that quantum fluctuations are not strong enough to destabilize a Néel state (at $T = 0$) – and why a kagome lattice is an even more favorable case to probe this conjecture. Indeed, in the triangular-based corner sharing geometry of the kagome lattice, the coordination number is only 4 as compared to 6 for the edge-sharing triangular lattice.

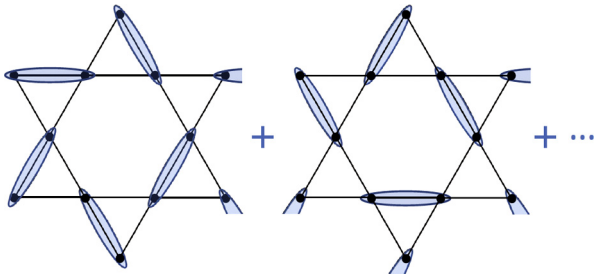

Fig. 3. The RVB intricate state made of all possible $2^{N/3+1}$ disordered pavings with singlet dimers on a kagome lattice of N $S = 1/2$ spins.

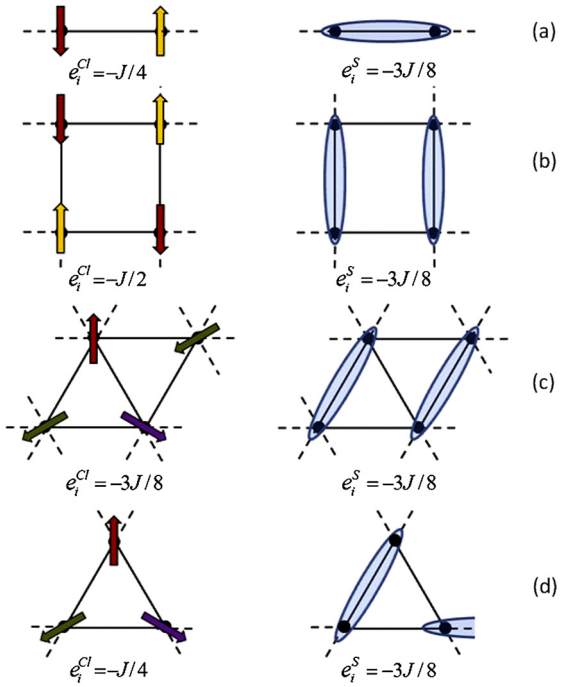

Fig. 4. Energy per spin for chains (a), square (b), triangular (c) and kagome lattices (d). Left: classical configurations and their energies e_i^{Cl}. Colors are for Néel sublattices. Right: dimer configurations and their energies e_i^{S}. Ellipses represent singlets. From F. Bert et al. [5].

Frustration is now a concept extending to much science, from protein folding [6], colloids [7], multiferroics [8] to emergent electromagnetism with the recent modeling of magnetic monopoles physics [9]. In this general spirit, Highly Frustrated Magnetism (HFM) appears as a novel playground and an incubator for new concepts combining frustration with the elegance of magnetic models. There, statistical or numerical-based theoretical methods and proof of concept materials are used to explore this new landscape.

In this paper, we will focus on the specific case of quantum spin liquids induced by frustration, which are one among the many topics that HFM encompasses [10].

1.2. Spin liquids: from 1D to the defeat of Néel state in higher dimension? A Grail quest

Combining three major ingredients, namely quantum fluctuations, geometric frustration and a weakly connected corner-sharing rather than edge-sharing lattice (see Fig. 4 and Fig. 5) indeed opens a novel avenue to exotic fluid-like states of matter, the so-called “spin liquids”: in the most naive picture, alike in a liquid, the constituent spins are still highly correlated at short distances, but fluctuate strongly down to absolute zero temperature. Such quantum spin liquids (QSL) were well identified and studied without the need of frustration in one dimension for more than 50 years. Unconventional fractional excitations were predicted and detected, they are no more spin-1 bosons, which usually characterize excitations classically viewed as spin waves but spin 1/2 excitations obeying a fermionic statistics [11].

Extending the spin liquid concept to 2D and 3D offers a complementary view to the idea of evading the Néel case. This has been inspiring theorists for long to study a variety of magnetic model Hamiltonians in which frustration is at play, but which can be far from experimental realizations. Such a spin liquid state had remained quite elusive experimentally until

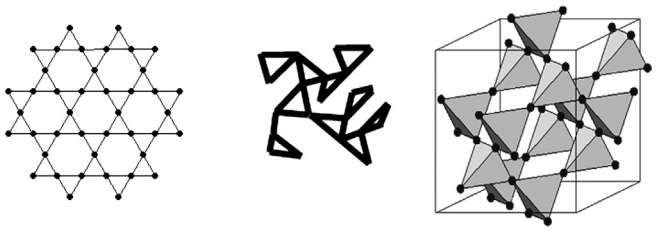

Fig. 5. Typical corner-sharing geometries. From left to right: kagome (2D), hyperkagome and pyrochlore (3D) lattices.

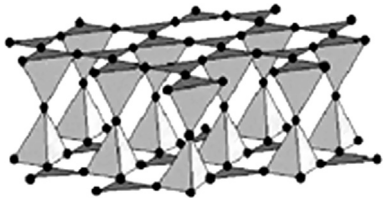

Fig. 6. Active magnetic structure [16] at low T in $SrCr_{9p}Ga_{12-9p}O_{19}$. Black circles are Cr^{3+}. Other atoms are not represented. Kagome bi-layers appear clearly.

a 2D kagome corner-sharing triangular-based cuprate material, named herbertsmithite, was first synthesized at M.I.T. [12], in 2005, and on which we, as many other groups, have intensively worked. In a quite recent review paper in *Nature* [13], L. Balents acknowledges the constantly increasing number of spin liquid candidate materials since then, which in turn has triggered a burst and a renewal of theoretical approaches and conceptual ideas.

Our paper is now divided into three parts. We first quickly review the early search for as simple a model compound as possible where a kagome QSL state can be stabilized. Some compounds have emerged and although finally stabilized into a frozen ground state, they showed specific signatures of an original state resembling that of a spin liquid: short coherence length, persisting dynamics in the frozen state. We will then make a short theoretical survey, from the experimentalists' point of view. Finally, we will detail the case of herbertsmithite, one of the few cases where a quantum spin liquid state is now clearly established on the simplest and most emblematic kagome lattice. We aim at describing the current status on the experimental side and place it in a perspective relative to state-of-the-art theoretical predictions.

2. Towards the kagome Heisenberg antiferromagnet: the first seeds

2.1. A first approach to novel facets of magnetism: the stone age

The idea for a resonating valence bond state was revived by Anderson in the context of the discovery of high-temperature superconductivity [14]. The idea was that hole doping in a CuO_2 antiferromagnetic plane could generate some frustration and lead to a resonating singlet dimer binding a hole and a Cu^{2+} spin. Tracing back to the original RVB ideas, this probably triggered the search for a more academic RVB proof of concept on antiferromagnetic triangular-based lattices.

Soon after indeed, the very first compound $SrCr_{9p}Ga_{12-9p}O_{19}$, $p = 0.89$, was investigated by Obradors et al., [15] and the first remarkable effects of frustration on a regular lattice were highlighted as detailed below. Its magnetically active structure consists of both kagome and triangular layers of Cr^{3+} ions [16], leading to a bi-plane geometry of corner sharing tetrahedra, so-called a pyrochlore slab, or kagome bi-layers (Fig. 6). It therefore features a not simple yet corner-sharing geometry, with half filled Cr^{3+}, ($3d^3$) t_{2g} orbitals, $S = \frac{3}{2}$, hence a negligible single ion anisotropy and a direct exchange coupling limiting the Hamiltonian to near-neighbor terms. All this leads to the realization of a quasi-perfect Heisenberg Hamiltonian on a corner-sharing lattice. Despite a Weiss temperature of ~ 500 K, a transition to a spin-glass-like phase was detected only at 3.5 K, the origin of which is still uncertain [17]. A frustration ratio defined as $f \sim \frac{\theta_W}{T_f}$ has been introduced by Ramirez [18], it reflects the decrease of the transition temperature due to frustration with respect to the mean-field characteristic temperature.[1] Specific heat [19] and muon spin relaxation measurements [20] emphasized the non-conventional character of this spin-glass state and pointed to the existence of exotic low-T dynamics in this compound, as somehow expected in a spin liquid on a corner sharing lattice, see section 3.

Jarosites was the other family heavily explored in the 90's [21]. They crystallize with a highly flexible structure, with the general formula $AB_3(SO_4)_2(OH)_6$ where the B^{3+} cation can be Fe^{3+} ($S = \frac{5}{2}$), Cr^{3+} ($S = \frac{3}{2}$) in the most studied cases and V^{3+} ($S = 1$). They provide a realization of classical kagome lattices where the effect of Dzyaloshinkii–Moriya anisotropy

[1] The concept of frustration ratio is more suited to 3D geometries than to the 2D case where a Néel order might, only be observed at $T = 0$ in the Heisenberg case.

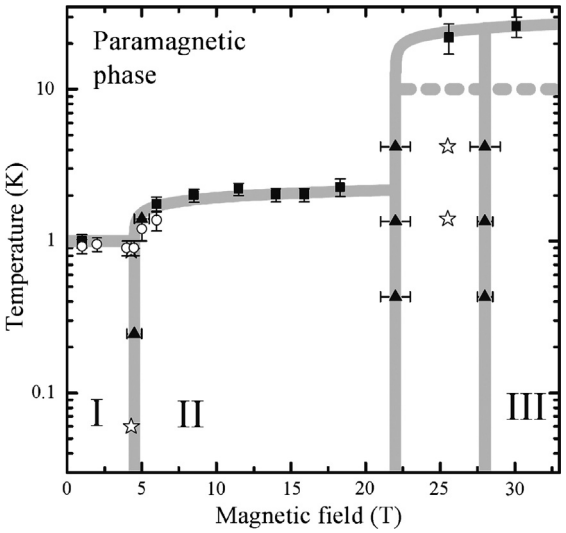

Fig. 7. Field phase diagram of volborthite ($J \sim 60$ K). The successive phases might reflect the physics of the anisotropic kagome lattice, but their structure is hard to determine from a local probe such as NMR. The present understanding is that phase I corresponds to a spin-density wave state (SDW), phase II is an inhomogeneous phase with both a SDW component and an ordered one with similar values of Cu moments, while in phase III the values of the moments differ.

was advocated to explain the Néel ordering observed in most cases [22]. This underlines the importance of additional perturbations. Frustration resulted in a large depression of the transition temperature, therefore a frustration ratio of a few tens.

2.2. The Cu^{2+} minerals track: the bronze and the iron ages

A second impetus to the field was given by what could be coined the Cu^{2+} minerals track. Copper (II) materials are natural candidates for realizing $S = 1/2$ quantum antiferromagnets, yet most of them form square-based networks, built from edge-sharing or corner-sharing CuO_4 square plaquettes. The kagome case has remained elusive for long, but the situation is far from hopeless and has progressed a lot since the early 2000s. Several compounds have now been isolated and have opened new experimental avenues with which to probe our understanding of kagome physics and have inspired new theoretical work. Z. Hiroi and collaborators proposed volborthite [23] $Cu_3V_2O_7(OH)_2{\cdot}2H_2O$ as the first representative of a kagome lattice decorated by Cu^{2+}. It soon appeared that a transition is detected at low temperature [24] and the most recent progress on this compound associating material science with NMR and high-field experiments underline that on a given triangle the magnetic bonds are non-equivalent, with maybe quite different strengths of interactions [25]. Why frustration is partially relieved and can lead to such a complex diagram as the one shown in Fig. 7 is still a matter of debate.

Herbertsmithite $ZnCu_3(OH)_6Cl_2$ was the first to feature a perfect equilateral geometry and the first kagome-layered compound to display no order down to $T = 0$. Other compounds or variants have been proposed since then. Close through their chemical formula but different on the magnetic ground, kapellasite [26] and haydeite [27] feature kagome lattices prone to illustrate frustration through the geometry of interactions rather than the geometry of the lattice. The first n.n. interactions are indeed ferromagnetic, while diagonal antiferromagnetic interactions are at the origin of competing effects. Kapellasite, which is a polymorph of herbertsmithite, turns out to be a spin liquid, while haydeite (Mg replaces Zn) has a ferromagnetic order. Finally vesignieite [28] $BaCu_3V_2O_8(OH)_2$ is the last example of a much less distorted kagome lattice than volborthite, but where ordering is also observed.

As one can understand, in this landscape, herbertsmithite appears as a unique representative. A full section will be devoted to describe its physics, which mirrors the intense activity on this compound. Why small perturbations lead to ordering in other compounds is still under study and a research avenue that will certainly shed light on the major instabilities of the spin liquid state. From these few examples, it appears that respecting the equilateral geometry is a serious constrain in view of finding $T \to 0$ spin-liquid-state materials.

2.3. Beyond Cu^{2+} minerals

Quite recently, other synthetic families of vanadium oxides have been proposed. $[NH_4]_2[C_7H_{14}N][V_7O_6F_{18}]$ [diammonium quinuclidinium vanadium(III,IV) oxyfluoride; DQVOF] is one member that contains a $S = 1/2$ KAFM network of V^{4+} d^1 cations. Despite significant antiferromagnetic exchange interactions, the system does not order at any investigated temperature. DQVOF contains two distinct vanadium sites, with V^{4+} $S = 1/2$ ions in the kagome layers and V^{3+} $S = 1$ ions between layers. An orbital coupling argument was put forward to suggest that the poor V^{4+}–V^{3+} superexchange pathway

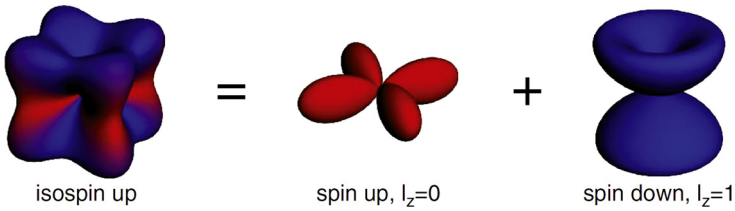

Fig. 8. Shape of the $J_{\text{eff}} = 1/2$ pseudo-spin state which admixes different t_{2g} orbitals and spin states as a result of spin orbit interaction $\lambda \vec{L}\cdot\vec{S}$ (from Ref. [31]).

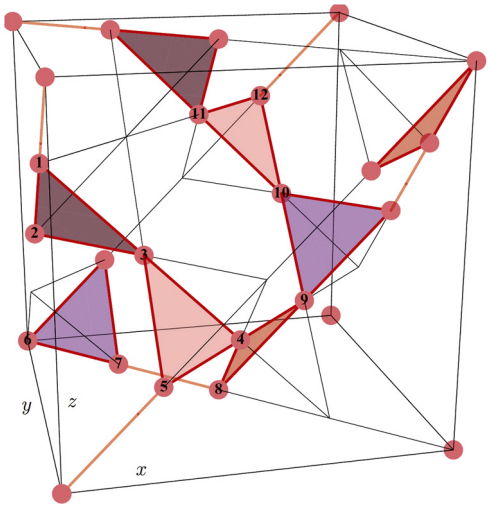

Fig. 9. Hyperkagome geometry as obtained by taking out 1 over 4 spins in a pyrochlore structure so as to get a corner-sharing structure.

within the structure should result in magnetically isolated $S = 1/2$ kagome planes at low temperatures [29]. DQVOF is therefore a good candidate QSL material displaying a gapless ground state [30] with reduced Jahn–Teller distortions with respect to the Cu^{2+} kagome systems, where they could impact the low-temperature magnetic properties.

In the strong spin–orbit limit, i.e. larger than the exchange interaction J, a condition that is easily met in iridates, the spin and orbital degrees of freedom are no longer independent, but bind together to form a complex combination as depicted in Fig. 8. In the case of Ir^{4+} with one hole per site, these pseudo-spin states are labeled by the total momentum $J_{\text{eff}} = 1/2$. When superexchange is projected onto the pseudo-spin space, the resulting Hamiltonian can differ substantially from the Heisenberg model. Along these lines, the ordered spinel compound $Na_4Ir_3O_8$ has triggered a lot of excitement as the very first example of a 3D quantum spin liquid where Ir^{4+} ions form an original "hyperkagome" 3D network of corner-sharing triangles [32] (Fig. 9). Recent experimental studies have shown that $Na_4Ir_3O_8$ has finally a transition to a disordered state with a frustration ratio $f \sim 90$ [33]. Furthermore, Na can be partially deintercalated, leading to a doped version of the hyperkagome lattice with $Na_3Ir_3O_8$ as an end member. Its properties are close to metallic [34] and start to be the focus of much attention.

3. Theoretical approaches to the KHAF problem

3.1. From classical to quantum

In an unfrustrated antiferromagnet, e.g., a simple cubic lattice with nearest neighbor exchange J described in a Heisenberg model, the lattice is bipartite, the classical ground states are two-sublattice Néel states with opposite directions of the magnetization for spins on different sublattices. This state is unique up to a global rotation that is a consequence of the symmetry of the Heisenberg Hamiltonian. Low-energy excitations are Goldstone modes, i.e. long-wavelength spinwaves that result from broken symmetry. Quantum fluctuations are also known to decrease the local magnetization (zero-point motion).

Moving to frustrated lattices without the quenched disorder characteristic of spin glasses, the triangular lattice would naturally lead to a tripartite lattice and a two-fold degeneracy that results from the choice of one of the two chiralities, one of which is shown in Fig. 2. In contrast, the corner-sharing geometry has a ground state manifold that is extensive although of smaller dimension than the high-dimensional phase space. It leads to a finite entropy per spin at $T = 0$. An elegant Maxwellian counting argument indicates that in the ground state there is an extensive number of degrees of freedom. Order by disorder processes select a coplanar spin configuration, and localized zero energy modes now appear [35]. This

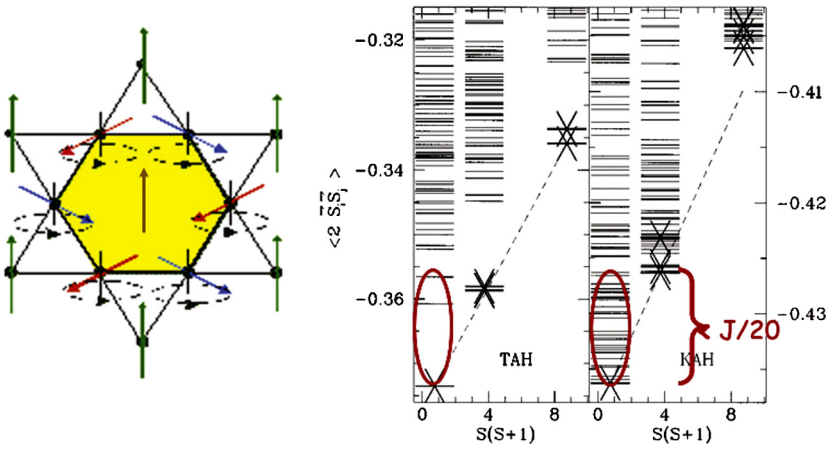

Fig. 10. Left: $\mathbf{q} = \sqrt{3} \times \sqrt{3}$ local modes on a classical kagome lattice with neighboring spins at 120°: coherent *local* rotation of spins belonging to two sublattices, around the direction of the third has no energy cost. Right: Energy spectrum using exact diagonalizations techniques. The striking difference between the triangular and kagome antiferromagnets, labeled TAH and KHAF, is the continuum of excitations in the singlet channel. The gap between the first singlet and triplet states is estimated at $\Delta < J/20$, if non-zero [37]. From Ref. [36].

situation can be viewed as a realization of cooperative paramagnetism that differs from simple paramagnetism where spins do not interact. The spin fluctuation time is no more set by J, but by $k_B T$, as observed in quantum critical phenomena [35].

Given the failure of Quantum Monte Carlo methods for triangular lattices, the spin 1/2 quantum case has been early approached through exact diagonalizations on small systems of N spins (N is now up to 48) [36–38]. Energies of the eigenstates can be sorted by the total spin value and thus build up towers of states. This is a rich construction from which one can extract important information about the existence of a broken symmetry or the existence of a singlet–triplet gap by extrapolation to the thermodynamic limit ($N \to +\infty$). Here, we simply use its results to illustrate the specific character of the corner- versus edge-sharing geometry. Clearly a continuum of excitations appears in both the singlet and triplet sectors only in the former case, which is the pendant of the classical soft modes (Fig. 10). We will come back to this method in the context of the next section.

These results, mostly established in the 1990s, clearly evidence the exceptional character of the corner-sharing geometry.

3.2. *Recent developments for the $S = 1/2$ kagome Heisenberg antiferromagnet: still an open debate!*

The question of the ground state of the KHAF is a long-pending issue that has been heavily debated without any definitive conclusion to date. The reason why is a competition between various types of solutions: they are so close in energy that the errors associated with the approximate treatments do not allow us to predict firmly which will be the winner, would all possible solutions be scrutinized. This is a consequence of the extensive quasi-degeneracy of the ground-state manifold.

The difficulty of finding the solution to this puzzle has stimulated development in theoretical and numerical techniques that are very successful in 1D for quantum magnets: among them, exact diagonalizations as already exemplified, up to 48 sites, series expansion, projected variational Monte Carlo, density matrix renormalization group (DMRG), Schwinger boson mean field theory, quantum dimer models, multiscale renormalization ansatz. Two classes of solutions have been explored.

Valence bond crystals All the spins are partitioned in specific localized valence bonds leading to a broken symmetry (see example in Fig. 11). Given the symmetries of the lattice, the smallest unit cells are made of 6, 12, and 36 sites. A spin gap between a singlet and a triplet state has been estimated to be $\Delta = 0.16\ J$ for the 36 sites unit cell "pinwheel" VBS [40]. The triplet excitations attract one another and form many bound states in the spin-singlet channel, many of which appear to lie below the spin gap in agreement with the results of exact diagonalizations.

Quantum spin liquids There are many possible spin liquid phases that have been classified along their symmetry and gauge invariance [41]. The most favorable from an energy point of view are listed below.

(i) Algebraic or U(1) Dirac spin liquid with fermionic excitations that one can view as a landmark of fractionalization and where the band structure consists of two Dirac cones [42]. Alike in a Fermi liquid, the ground state is gapless and spin–spin correlations decay as a power law. This phase is very sensitive to perturbations, such as anisotropy and therefore appears to be marginally stable and is coined "critical". It might destabilize into an ordered phase or into valence-bond crystals that both break the symmetry. Yet recent projected wave function variational methods indicate that without such a perturbation, this gapless phase is a solid proposal [43].

(ii) Uniform RVB spin liquid which is also a gapless U(1) spin liquid, but where the band structure consists of a circular spinon Fermi surface [44].

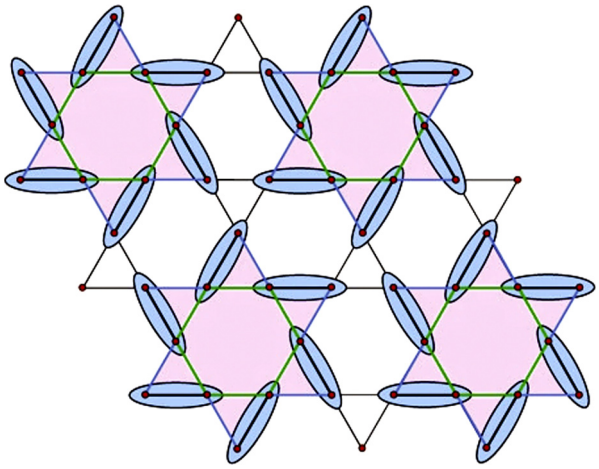

Fig. 11. "Pinwheel" VBS ground state in the $S = 1/2$ deformed kagome lattice antiferromagnet $Rb_2Cu_3SnF_{12}$[39].

(iii) Chiral and $\mathbb{Z}_2$ spin liquids are gapped states and belong to the category of short-range RVB spin liquids [45,46]. The DMRG calculations, well known to be very efficient in the 1D limit, have been extended to the quasi-2D limit on cylinders with kagome boundary conditions on the perimeter [46]. They were a major achievement in the field and support a $\mathbb{Z}_2$ spin liquid phase with a gap whose value is still highly debated. Initially thought to be of the order of 0.2 J, it is now better estimated through various geometries to be in the range of 0.05–0.1 J [47,48]. Very recently, the combination of high-temperature series expansion and entropy constraints point to a value of the spin gap as low as 0.03 J [49].

One striking result of all these approaches is that all the ground-state energies are very close, with an energy per site of -0.42866 J for the U(1) algebraic spin liquid [42] and -0.4386 J for the fully gapped $\mathbb{Z}_2$ non-chiral spin liquid [47]!

Of course, one of the crucial issues for experimentalists is to know (i) which are the observables that will discriminate between the various proposals, the gapped character is certainly one, and (ii) what could be the deviations to the Heisenberg Hamiltonian (anisotropy, magnetic or non-magnetic substitutions, Zeeman term under the control of an external field) and to the ideal geometry of interactions (further neighbors, distorted geometry) in the realm of materials.

Prior to any spin liquid exploration, a prerequisite is to know whether some freezing occurs and possibly restricts the study of the spin-liquid state to an appropriate finite T-range. Transitions that can be marginal are in most cases difficult to detect with macroscopic techniques and for this, muon spin resonance, μSR, is a quintessential technique[2] that is capable of revealing tiny fractions of a Bohr magneton of static (frozen or ordered) magnetism. Neutrons can be used but with a far less suited sensitivity especially for 1/2 spins. Obviously, magnetic susceptibility, T_1 measurements that probe the low-lying magnetic excitations and neutron scattering measurements that probe higher energy excitations are prone to discriminate between spin-gapped and gapless ground states. Specific heat, Raman scattering and infra-red absorption probe all excitations, including those in the singlet channel. Electronic spin resonance is an invaluable technique for determining anisotropic interactions.

4. Herbertsmithite: a near-perfect KHAF experimental realization

4.1. Herbertsmithite as a member of the paratacamite family

Herbertsmithite $ZnCu_3(OH)_6Cl_2$, a rare mineral recently extracted and named after G.F. Herbert Smith (1872–1953), who discovered the mother paratacamite family in 1906 [52], has been synthesized for the first time in 2005, in M.I.T. [12] and soon after in Europe by groups we have been collaborating with. It has triggered a major renewal in the search of a quantum spin liquid on the KHAF lattice and opened the possibility to directly expose theories to experiments for the KHAF ground state.

Herbertsmithite is the $x = 1$ end-compound of the Zn-paratacamite family $Zn_xCu_{4-x}(OH)_6Cl_2$ [12,53,54]. It can be viewed as a double variant of the parent clinoatacamite compound ($x = 0$), a Jahn–Teller distorted $S = 1/2$ pyrochlore. The symmetry first relaxes from monoclinic ($P2_1/n$) to rhombohedral ($R\bar{3}m$) around $x = 0.33$, leading to a perfect kagome lattice in the a–b plane with isotropic planar interactions, $J \sim 170$ K; then, in the c-elongated $x > 0.33$ pyrochlore structure, the magnetic bridge along the c-axis between a–b kagome planes is progressively suppressed by replacing the apical Cu^{2+} by a

[2] μSR is a large scale facility experiment (ISIS, UK, PSI, Switzerland, in Europe). Fully polarized μ^+, $S = 1/2$ beams are implanted in any material, their precession in a field can be traced through their disintegration in positrons. For an introduction, see [50]. For a deeper approach, see [51].

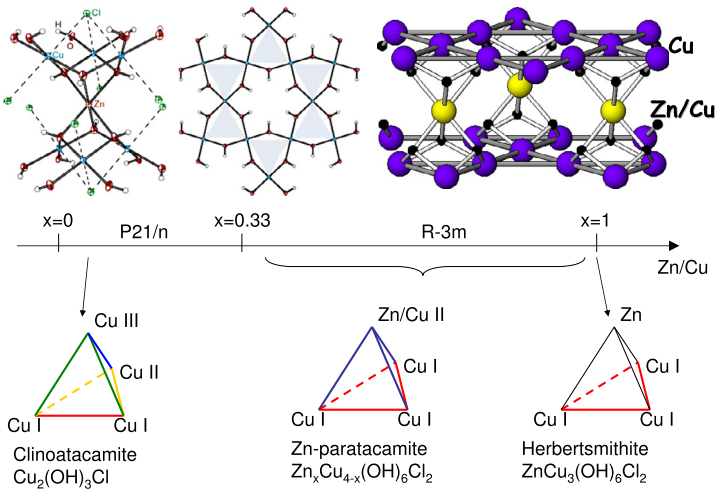

Fig. 12. Top left: structure of Herbertsmithite from [12]. Top right: simple sketch of the structure where only Zn and Cu sites have been represented. Bottom: Evolution of the structure of paratacamites when Zn content is increased. A structural transition occurs around $x = 0.33$ which yields well defined perfect kagome planes, assumed to be filled with Cu only.

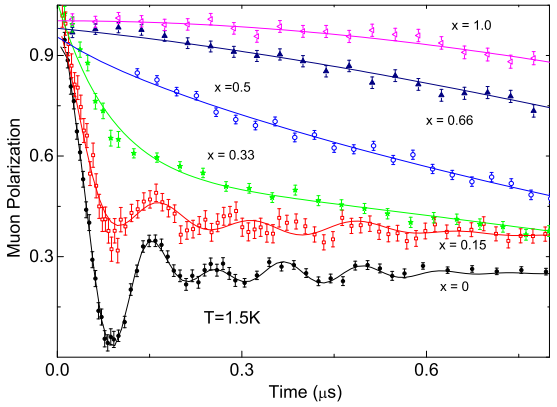

Fig. 13. Evolution of the low-T μSR asymmetry when Zn content is progressively increased. The oscillations due to the existence of well defined static fields progressively disappear and, for $x > 0.5$, the frozen magnetism disappears. (Adapted from [59].)

diamagnetic Zn^{2+}. Due to a more favorable electrostatic environment, Cu^{2+} is expected to preferentially occupy the distorted octahedral kagome sites only. Ideally, when $x = 1$ the $S = 1/2$ ions should therefore form structurally perfect kagome layers that are themselves well separated by diamagnetic Zn^{2+} (Fig. 12). It is now clearly established from susceptibility [55], magnetization measurements [56], Schottky anomalies in the low-T specific heat [57], anomalous X-ray diffraction [58] that the inter-layer site is randomly occupied by 20–30% Cu^{2+}, yet with a negligible coupling with the kagome planes J' at most of 1 K $\sim 0.006\ J$. This has zero/weak incidence on the physics of the kagome planes, but a severe impact on the experimental observables. These quasi-free spins indeed completely dominate the thermodynamic quantities at low T – for example a $T \to 0$ diverging Curie tail that dominates the kagome susceptibility – which has made them of much less direct relevance to probe the physics of the kagome planes.

4.2. A quantum spin liquid!

Owing to its extreme sensitivity to static frozen phases, zero-field μSR experiments enable us to track in minute details the magnetism of the entire paratacamite family [59]. For intermediate Zn contents $0.33 < x < 0.66$, the low-temperature phase appears to be locally inhomogeneous, which translates into two components in the μSR signal; one from a frozen magnetic environment reminiscent of the ordered phase in clinoatacamite (frustration ratio ~ 12) that gets more and more disordered as x increases, and one from a dynamical environment of the muon (Fig. 13). The evolution of this frozen fraction detected in μSR yields the phase diagram plotted in Fig. 14. Interestingly, for $x > 0.66$, the frozen fraction gets lower than the experimental accuracy (a few percent) and a fully "liquid" phase appears, although 1/3rd of the inter-layer 3D coupling paths are still active.

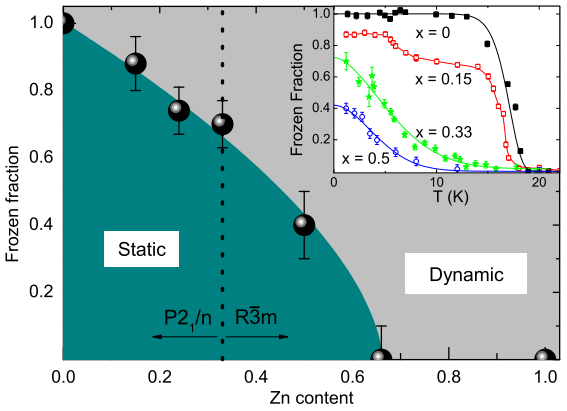

Fig. 14. Phase diagram of the paratacamite family as deduced from the $T \to 0$ frozen fractions found in zero-field μSR experiments [59] (inset).

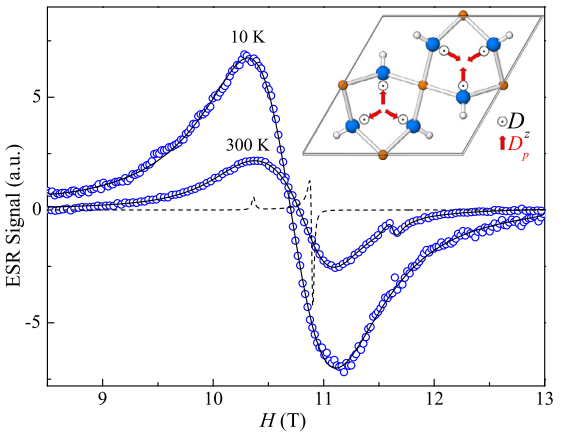

Fig. 15. ESR spectra taken at 300 and 10 K. The broad linewidth is due to a large anisotropy. The dashed line shows the anisotropy of the g- shift tensor, hence the minute deviation from a pure Heisenberg character of the spins, quite common for Cu^{2+} ions. In the inset the Dzyaloshinskii vectors are represented. The Cu and O are respectively represented by small and large full circles (red and blue). Adapted from Ref. [60].

The large domain of stability of a "liquid" phase in the phase diagram of paratacamites is certainly a consequence of both the weak inter-layer coupling and the shortness of the in-plane correlation length. No magnetic freezing has ever been observed in the $x = 1$ compound down to our lowest probed temperature of 20 mK through μSR [59]. The upper bound value of a hypothetical frozen moment would then be less than $6 \times 10^{-4} \mu_B$ (μSR). This is completely consistent with ac susceptibility results for $x = 1$, which behaves monotonously down to the lowest temperature (50 mK) and with neutron scattering where no magnetic diffraction Bragg peak was detected at variance with clinoatacamite [55].

Herbertsmithite therefore appears as the first structurally perfect kagome antiferromagnet not displaying any magnetic transition. This has opened wide the field of experimental investigations of the quantum spin-liquid behavior down to $T = 0$ in kagome antiferromagnets.

4.3. Is herbertsmithite "the" perfect KHAF?

Anisotropies Due to the lack of inversion symmetry between two adjacent Cu, spin–orbit coupling yields an antisymmetric Dzyaloshinkii–Moriya interaction $\vec{D}_{ij} \cdot \vec{S}_i \times \vec{S}_j$ which adds up to the Heisenberg Hamiltonian. $\vec{D}$ has two components, one perpendicular to the planes, D_z, and one planar D_p. ESR is one of the most appropriate techniques to investigate such local spin anisotropies even on powders where a broad linewidth at 300 K supports the existence of such anisotropy (Fig. 15). Attributing all the ESR linewidth to this DM anisotropy yields an upper bound estimate of $D_p \sim 0.01 J$ (negligible) and sizable $D_z \sim 0.04$–$0.08 J$ [60,61], a common value in Cu oxides.

At variance with the already discussed classical case where any minute amount of DM anisotropy will lead to long-range order [22], studies of the phase diagram of a quantum Heisenberg kagome lattice with DM interactions shows that an original spin-liquid phase can survive and indeed, herbertsmithite is in this case. For spins $S = 1/2$, a quantum critical point indeed appears for $D/J \sim 0.1$, which separates the liquid and the Néel states [62–64]. These results are sketched in Fig. 16.

The first synthesis of single crystals by M.I.T., a major achievement of recent years, has given a new look upon the anisotropies [65]. The analysis of the high-T susceptibility suggests an anisotropy in Heisenberg exchange interactions of

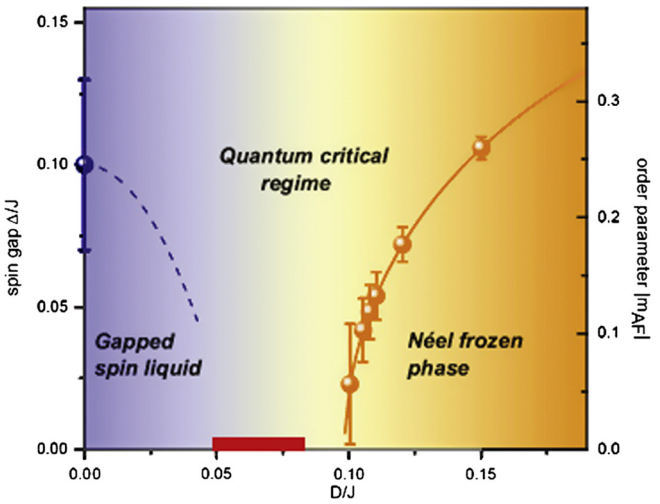

Fig. 16. Theoretical $T = 0$ phase diagram of the KHAF as a function of the strength of DM interaction, D/J. The Néel order parameter has been calculated by exact diagonalizations. The spin gap in the spin liquid phase is issued from DMRG calculations while the dashed line gives a sketch of its evolution. Adapted from Ref. [5].

the order of 0.1 J, but g factor anisotropies from that analysis seem to be too high to fit with the ESR results. Attributing the whole ESR linewith to such an anisotropy rather gives an upper bound of 0.06 J [66]. One can certainly conclude that such anisotropies are both present and constitute one of the major deviations to the Heisenberg model that has to be kept in mind in the comparison between models and low-T experimental results.

Further-neighbor interaction This is a deviation to the Heisenberg model which has been up to now overlooked. Kapellasite, a polymorph of herbertsmithite, has a very similar kagome plane structure where Cu–OH–Cu bonds and angles vary little with respect to Herbertsmithite [67,68]. Although this has a drastic effect on the first-neighbors interaction that switches from anti- to ferro-magnetic, it is interesting to consider further neighbor interactions that should be very similar in the two compounds. The second neighbor one appears to be a negligible correction as compared to the along-diagonal of the hexagon antiferromagnetic interaction $\sim$0.1 J [69]. One can note that this adds up to the NN frustrating interaction and should not therefore much impact a potential spin-liquid behavior.

Anti-site mixing? Finally, we have already mentioned the occupation of the Zn site by Cu. There is a still open debate between the possibility of intersite mixing leading to a $\sim$6% spin vacancies in the kagome planes and defectless kagome planes. While the former has been suggested by intra-plane local ^{17}O NMR measurements [70] on powder samples, X-ray anomalous scattering on single crystals speaks in favor of full occupancy, i.e. perfect kagome planes, which somehow contradicts the perfect stoichiometry deduced from ICP–AES experiments on the same samples [58]. In any case, as far as we know, such a weak level of dilution in the kagome lattice should not alter its fundamental properties.

Conclusion One can safely argue that deviation to the Heisenberg case occurs at a maximum level of 0.1 J. This calls for some care in interpreting experiments with existing models and is a clear signal that given the low symmetry of kagome compounds, a test of theoretical models along these perturbations is likely the next step to undertake.

4.4. A gapless ground state?

Given the dominant contribution of out of plane defects in macroscopic measurements, only site-selective probes can give some insight into the thermodynamic response of the kagome planes. There are certainly two ideal probes of the kagome susceptibility, Cu and O nuclei. Unfortunately, Cu has never been detected in the whole T-range and the detection of a signal that was reported in [72] is certainly encouraging, but whether Cu, either in-plane or out-of-plane, is detected is still an open question. O therefore appears to be the most secure probe. From a simple comparison to other probes at high-T, where the macroscopic susceptibility is dominated by the kagome planes, O is found to be one order of magnitude at least better coupled than Cl [72] and two orders of magnitude better than implanted muons in μSR experiments [73].

4.4.1. Kagome susceptibility from ^{17}O NMR [70,71]

Tracking the position of the main resonance [70] gives the shift, hence one can extract the hereafter called "intrinsic" susceptibility from 300 K $\sim$ 1.7 J down to 0.45 K $\sim J/400$. A broad maximum is observed between the high-T Curie–Weiss regime and the low-T regime where the susceptibility monotonously decreases between $J/3$ and $J/20$ to finally level-off at a finite value within error bars. The latter are quite large at low-T given a sizable defect-induced line broadening so that this

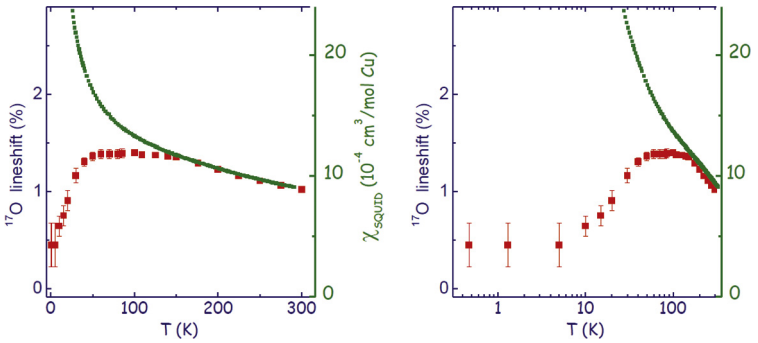

Fig. 17. Thermal variation of the susceptibility of the kagome planes measured from the shift of the main ^{17}O NMR line (red open symbols) compared to the macroscopic susceptibility (green solid line). The red dashed line is a guide to the eye for the low-T shift.

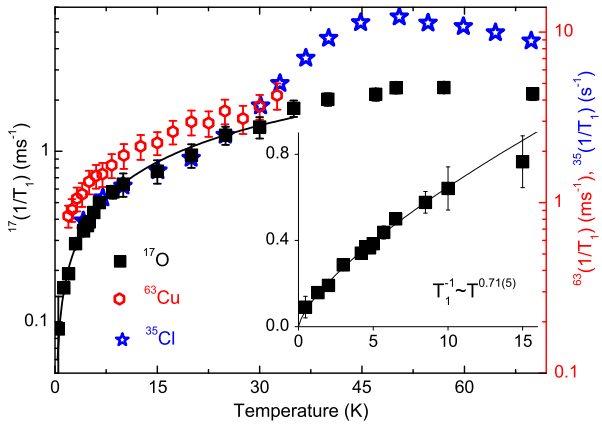

Fig. 18. Semi-log plot of the relaxation rates obtained for all probe nuclei, ^{17}O, ^{63}Cu and ^{35}Cl. Inset: linear plot of T_1^{-1} with a power law fit for the low T ^{17}O data. Adapted from Ref. [70,72].

data should rather be taken with some care. The behavior in the intermediate T-range can certainly be associated with a strengthening of the short-range antiferromagnetic correlations. Fig. 17 illustrates the huge difference between the intrinsic susceptibility of the kagome planes and the macroscopic susceptibility, which is dominated at low T by the inter-plane defects. The finite value of the susceptibility, if further confirmed, could be attributed to a singlet–triplet mixing induced by DM interactions. Yet, using the DM calculations in a dimer model [74] gives a strong indication that the DM interaction is not in an obvious manner the origin of the non-zero susceptibility at $T = 0$ and might point to an intrinsic gapless ground state for the KHAF. This calls for further realistic inclusions of the DM interaction into the kagome Heisenberg Hamiltonian.

Given the uncertainty on the low-T behavior of the susceptibility, the best way to probe the existence of a gap is to turn to the dynamical susceptibility measurements.

4.4.2. Dynamical susceptibility and exotic excitations

Both NMR T_1 relaxation measurements [70,72] (Fig. 18) and inelastic neutron scattering (INS) [55,75] give also a strong support to a gapless scenario, at least in the field and temperature ranges that have been probed.

NMR T_1 measurements taken using various probes agree well from 30 K down to 1.2 K clearly pointing to gapless magnetic excitations with a power law behavior $T_1^{-1} \sim T^{0.71(5)}$.

INS data have been taken without any applied field down to 35 mK on powders [55] and down to 1.6 K on single crystals [76] synthesized at M.I.T., a major achievement of recent years. They consistently reveal that no gap larger than 0.1 J can be detected in any direction of the Q-space. Per se, this is already a very strong result as one might expect that only some directions of the reciprocal space could be gapless but the most striking result is the indication of a spinon-like continuum of excitations. While conventional spin-wave excitations take the form of sharp surfaces of dispersion in Q–ω space, in herbertsmithite, no surfaces of dispersion are observable in the low-temperature data, which provides a direct evidence that the excitations are fractionalized, forming a continuum. With the exotic T_1 power law, this can be taken as two solid experimental milestones that certainly need further refinements, but already indicate that herbertsmithite is a fantastic experimental playground for the QSL concept in 2D.

Finally Raman spectroscopic investigations of the quasi-elastic signal [77] indicate that the magnetic energy density of excitations obeys a power-law dependence with T and the in-plane low-frequency optical conductivity [78] has a power-law ω dependence. Both indicate a gapless ground state consistent with a U(1) spin liquid.

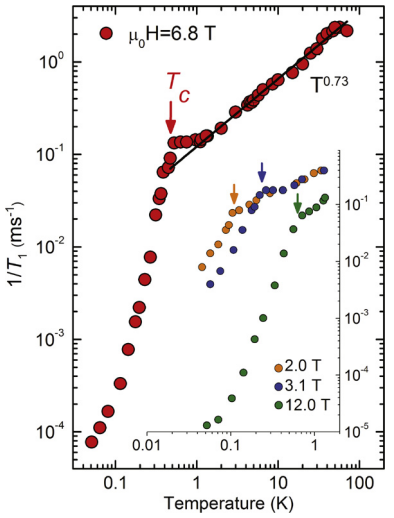

Fig. 19. T-dependence of the NMR relaxation rate under a magnetic field of 6.8 Teslas. Inset, the same for 2, 3.1 and 12 Teslas. A drastic decrease of the relaxation rate is observed below a temperature T_c that increases with the applied field.

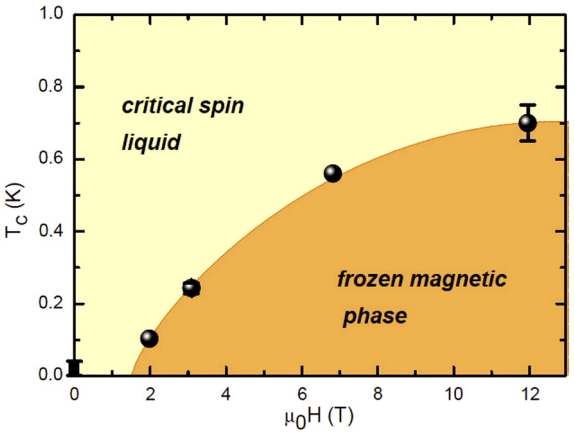

Fig. 20. T–H phase diagram. Circles are for NMR-detected transitions (Fig. 19) while the square symbol stands for the absence of transition established by μSR.

4.5. Field-induced freezing

We have underlined the plausible impact of perturbations on the ground state of the KHAF. DM anisotropy is one example, see above. Pressure, as proven experimentally, is another one with a transition to a Néel state at a moderate 2.5 GPa pressure. However, no clear idea emerges about the modification of structural parameters and their impact on the physics [79]. Given that strong frustration generates a downward shift of the excitations energy, it is interesting to probe the effect of an applied magnetic field on the low T physics. A drastic slowing down of the low-energy dynamics to a static phase is observed at a temperature T_c that depends on the field value (Fig. 19) and is characterized by a weak value of the Cu^{2+} moment [80]. This gives the T–H phase diagram displayed in Fig. 20 where a field onset of the "solid" phase occurs at 1.5 Tesla. This corresponds to a very small energy scale $\sim$1 K as compared to J. This sets another critical line marking the transition from a gapless spin liquid to a gapped static state in herbertsmithite.

4.6. A short comparison to models: a stumbling puzzle

From an experimental point of view, herbertsmithite displays a gapless spin liquid phase under zero field, which turns into a frozen state with a tiny gap under an applied field. All this could argue in favor of a gapless model against most of the recent DMRG results. The latter support an RVB state with indeed a small gap, at worse of the order of 5 K, within reach of all experiments. Would it be the lowest in energy, the U(1) Dirac model would provide an ideal framework to be compared to. Both a quantitative T-dependence of the susceptibility similar to what is observed and a power law for the T-dependence of T_1 are rewarding outputs of such a model but, as underlined in sec. 3.2, it is very sensitive to perturbation

terms as Zeeman effect (which would go the right way!) and anisotropy, which naturally destabilizes it into an ordered phase.

There are therefore two ways to reconcile the herbertsmithite case with theories: either the gapped phase is not evident because of the singlet–triplet mixing due to DM anisotropy or herbertsmithite is close to a quantum critical point because of DM anisotropy or else to be dug out, and quantum criticality dominates its experimental properties.

Note added after revision of the paper A new ^{17}O NMR study has recently reported data on herbertsmithite single crystals [82]. This enables the authors to reach an unprecedented accuracy on the shift, resolve the spectral contribution from the defect(s) site and perform a site-selective T_1 study. While a $J/10$ gap under zero-field is claimed which would contradict our conclusions, more discussions on this result are needed in our opinion which are beyond the scope of this paper, such as the presence of a large contribution to T_1 attributed by the authors to Cu/Zn defects.

5. Conclusion

Herbertsmithite is the first 2D compound with a corner-sharing geometry where frustration plays a major role to amplify quantum fluctuations and give birth to novel quantum states that feature a spin-liquid behavior. The comparison of experimental results with existing and still improving theories requests a refined understanding of the (small) deviations to the Heisenberg model that enter the game when $T \to 0$. The synthesis of high-quality single crystals where microscopic parameters can be controlled is a promising new era that has just opened. In return, the theoretical study of such perturbations will shed a new light on the physics of spin liquids. It is interesting to point out that spinless defects in the KHAF, back to the Friedel spirit, might act as a revelator of the underlying physics [81], which is a promising track for future studies.

Herbertsmithite is to-date one example among a few ones maybe in a less canonical context than the Heisenberg model limited to near-neighbor interactions: multiple competing interactions, non-kagome geometries, strong spin–obit coupling where iridates seem to be at the forefront of experimental explorations with the additional exciting possibility of charge doping “à la RVB”.

There is no doubt that recent years have seen decisive and constant progress in the field of quantum spin liquids in dimension higher than one. Even more is to be expected in years to come to move from our present view in the field and its challenging puzzles to a state-of-the art understanding just like in 1D quantum magnetism.

Acknowledgements

Our work presented in this paper was supported by the French Agence Nationale de la Recherche under Grants Nos. ANR-OxyFonda-05-4-41913, ANR-HFM-09-JCJC-0093-01, ANR-SpinLiq-12-BS04-0021-01, Université Paris-Sud Grant MRM PMP, JSPS KAKENHI Grant No. 25800188, by European Commission under EC FP 6 program, Contract No. RII3-CT-2003-505925 for the work at PSI and ISIS, PHC Proteus No. 24322SF, European Commission MC Grant No. MEIFCT-2006-041243, ARRS Project No. Z1-9530. NHMFL is supported by NSF (No. DMR-0654118) and the State of Florida.

References

[1] For a review, see K.H. Fischer, J.A. Hertz, Spin Glasses, Cambridge University Press, 1993.
[2] K. Binder, in: J. Treusch (Ed.), Festkörperprobleme, in: Advances in Solid State Physics, vol. 17, Springer, 1977, p. 55.
[3] G. Toulouse, Commun. Phys. 2 (1977) 115.
[4] P.W. Anderson, Mater. Res. Bull. 8 (1973) 153;
P. Fazekas, P.W. Anderson, Philos. Mag. 30 (1974) 423.
[5] F. Bert, P. Mendels, O. Cépas, C. Lhuillier, Reflets Phys. 37 (2014) 4.
[6] J.N. Onuchic, Z. Luthey Schulten, P.G. Wolynes, Annu. Rev. Chem. 48 (1997) 545–600.
[7] For example, Y. Han, Y. Shokef, A.M. Alsayed, P. Yunker, T.C. Lubensky, A.G. Yodh, Nature 456 (2008) 898.
[8] For example, S.-W. Cheong, M. Mostovoy, Nat. Mater. 6 (13) (2007).
[9] C. Castelnovo, R. Moessner, S.L. Sondhi, Nature 451 (2008) 42;
S.T. Bramwell, M.J.P. Gingras, Science 294 (2001) 1495;
S.T. Bramwell, et al., Nature 461 (2009) 956;
T. Fennell, et al., Science 326 (2009) 415.
[10] C. Lacroix, P. Mendels, F. Mila, Introduction to Frustrated Magnetism, Springer Series in Solid-State Sciences, vol. 164, Springer, Berlin, 2011.
[11] J. des Cloizeaux, J.J. Pearson, Phys. Rev. 128 (1962) 2131;
M. Mourigal, et al., Nat. Phys. 9 (2013) 435.
[12] M.P. Shores, E.A. Nytko, B.M. Barlett, D.G. Nocera, J. Am. Chem. Soc. 127 (2005) 13462.
[13] L. Balents, Nature 464 (2010) 199–208.
[14] P.W. Anderson, Science 235 (1196) (1987).
[15] X. Obradors, A. Labarta, A. Isalgue, J. Tejada, J. Rodriguez, M. Pernet, Solid State Commun. 65 (1988) 189;
B. Martínez, A. Labarta, R. Rodríguez-Solá, X. Obradors, Phys. Rev. B 50 (2014) 15779.
[16] S.-H. Lee, C. Broholm, G. Aeppli, T.G. Perring, B. Hessen, A. Taylor, Phys. Rev. Lett. 76 (1996) 4424.
[17] A. Sen, K. Damle, R. Moessner, Phys. Rev. B 86 (2012) 205134;
A. Sen, K. Damle, R. Moessner, Phys. Rev. Lett. 106 (2011) 127203;
L. Limot, et al., Phys. Rev. B 65 (2002) 144447.
[18] K.H.J. Buschow (Ed.), Handbook of Magnetic Materials, vol. 13, Elsevier Science, 2001, pp. 423–520.
[19] A.P. Ramirez, G.P. Espinosa, A.S. Cooper, Phys. Rev. Lett. 64 (1990) 2070.

[20] Y.J. Uemura, et al., Phys. Rev. Lett. 73 (1994) 3306.
[21] P. Mendels, A.S. Wills, in: C. Lacroix, P. Mendels, F. Mila (Eds.), Introduction to Frustrated Magnetism, in: Springer Series in Solid-State Sciences, vol. 164, Springer, Berlin, 2011.
[22] M. Elhajal, B. Canals, C. Lacroix, Phys. Rev. B 66 (2002) 014422.
[23] Z. Hiroi, et al., J. Phys. Soc. Jpn. 70 (2001) 3377.
[24] F. Bert, D. Bono, P. Mendels, F. Ladieu, F. Duc, J.-C. Trombe, P. Millet, Phys. Rev. Lett. 95 (2005) 087203.
[25] M. Yoshida, M. Takigawa, S. Krämer, S. Mukhopadhyay, M. Horvatic, C. Berthier, H. Yoshida, Y. Okamoto, Z. Hiroi, J. Phys. Soc. Jpn. 81 (2011) 024703, references therein.
[26] B. Fåk, E. Kermarrec, L. Messio, B. Bernu, C. Lhuillier, F. Bert, P. Mendels, B. Koteswararao, F. Bouquet, J. Ollivier, A.D. Hillier, A. Amato, R.H. Colman, A.S. Wills, Phys. Rev. Lett. 109 (2012) 037208;
B. Bernu, C. Lhuillier, E. Kermarrec, F. Bert, P. Mendels, R.H. Colman, A.S. Wills, Phys. Rev. B 87 (2013) 155107.
[27] D. Boldrin, B. Fak, M. Enderle, S. Bieri, J. Ollivier, S. Rols, P. Manuel, A.S. Wills, Phys. Rev. B 91 (2015) 220408(R).
[28] Y. Okamoto, H. Yoshida, Z. Hiroi, J. Phys. Soc. Jpn. 78 (2009) 033701;
R.H. Colman, F. Bert, D. Boldrin, A.D. Hillier, P. Manuel, P. Mendels, A.S. Wills, Phys. Rev. B 83 (2011) 180416(R);
J.A. Quilliam, F. Bert, R.H. Colman, D. Boldrin, A.S. Wills, P. Mendels, Phys. Rev. B 84 (2011) 180401(R);
M. Yoshida, Y. Okamoto, M. Takigawa, Z. Hiroi, J. Phys. Soc. Jpn. 82 (2013) 013702.
[29] F.H. Aidoudi, D.W. Aldous, R.J. Goff, A.M.Z. Slawin, J.P. Attfield, R.E. Morris, P. Lightfoot, Nat. Chem. 3 (2011) 801–806.
[30] L. Clark, J.C. Orain, F. Bert, M.A. De Vries, F.H. Aidoudi, R.E. Morris, P. Lightfoot, J.S. Lord, M.T.F. Telling, P. Bonville, J.P. Attfield, P. Mendels, A. Harrison, Phys. Rev. Lett. 110 (2013) 207208.
[31] G. Jackeli, G. Khaliullin, Phys. Rev. Lett. 102 (2009) 017205.
[32] Y. Okamoto, et al., Phys. Rev. Lett. 99 (2007) 137207.
[33] A.C. Shockley, F. Bert, J.-C. Orain, Y. Okamoto, P. Mendels, Phys. Rev. Lett. 115 (2015) 047201.
[34] T. Takayama, et al., Sci. Rep. 4 (2014) 6818.
[35] J. Chalker, in: C. Lacroix, P. Mendels, F. Mila (Eds.), Introduction to Frustrated Magnetism, in: Springer Series in Solid-State Sciences, vol. 164, Springer, Berlin, 2011.
[36] P. Lecheminant, B. Bernu, C. Lhuillier, L. Pierre, P. Sindzingre, Phys. Rev. B 56 (1997) 2521;
C. Waldtmann, H.U. Everts, B. Bernu, C. Lhuillier, P. Sindzingre, P. Lecheminant, L. Pierre, Eur. Phys. J. 2 (1998) 501–507.
[37] P. Sindzingre, C. Lhuillier, Eur. Phys. Lett. 88 (2009) 27009.
[38] Andreas M. Läuchli, Julien Sudan, Erik S. Sørensen, Phys. Rev. B 83 (2011) 212401.
[39] K. Morita, et al., J. Phys. Soc. Jpn. 77 (2008) 043707;
T. Ono, et al., Phys. Rev. B 79 (2009) 174407.
[40] Rajiv R.P. Singh, David A. Huse, Phys. Rev. B 77 (2008) 144415.
[41] X.G. Wen, Phys. Rev. B 65 (2002) 165113.
[42] Y. Ran, M. Hermele, P.A. Lee, X.-G. Wen, Phys. Rev. Lett. 98 (2007) 117205;
M. Hermele, Y. Ran, P.A. Lee, X.-G. Wen, Phys. Rev. B 77 (2008) 224413;
M.B. Hastings, Phys. Rev. B 63 (2000) 014413.
[43] Y. Iqbal, F. Becca, D. Poilblanc, New J. Phys. 14 (2012) 115031;
Y. Iqbal, F. Becca, S. Sorella, D. Poilblanc, Phys. Rev. B 87 (2013) 060405(R).
[44] O. Ma, J.B. Marston, Phys. Rev. B 101 (2008) 027204.
[45] L. Messio, B. Bernu, C. Lhuillier, Phys. Rev. Lett. 108 (2012) 207204.
[46] S. Yan, D.A. Huse, S.R. White, Science 332 (2011) 1173.
[47] S. Depenbrock, et al., Phys. Rev. Lett. 109 (2012) 067201.
[48] S. Nishimoto, N. Shibata, C. Hotta, Nat. Commun. 4 (2013) 2287.
[49] B. Bernu, C. Lhuillier, Phys. Rev. Lett. 114 (2015) 057201.
[50] S.J. Blundell, Contemp. Phys. 40 (1999) 175–192.
[51] A. Yaouanc, P. Dalmas de Réotier, Muon Spin Rotation, Relaxation, Resonance, Oxford University Press, 2010.
[52] R.S.W. Braithwaite, K. Mereiter, W. Paar, A. Clark, Mineral. Mag. 68 (2004) 527.
[53] P. Mendels, F. Bert, J. Phys. Soc. Jpn. 79 (2009) 011001.
[54] J. Phys. Conf. Ser. 320 (2011) 012004.
[55] J.S. Helton, K. Matan, M.P. Shores, E.A. Nytko, B.M. Bartlett, Y. Yoshida, Y. Takano, A. Suslov, Y. Qiu, J.H. Chung, D.G. Nocera, Y.S. Lee, Phys. Rev. Lett. 98 (2007) 107204.
[56] F. Bert, S. Nakamae, F. Ladieu, D. L'Hote, P. Bonville, F. Duc, J.-C. Trombe, P. Mendels, Phys. Rev. B 76 (2007) 132411.
[57] M.A. de Vries, K.V. Kamenev, W.A. Kockelmann, J. Sanchez-Benitez, A. Harrison, Phys. Rev. Lett. 100 (2008) 157205.
[58] D.E. Freedman, T.H. Han, A. Prodi, P. Müller, Q.-Z. Huang, Y.-S. Chen, S.M. Webb, Y.S. Lee, T.M. McQueen, D.G. Nocera, J. Am. Chem. Soc. 132 (2010) 16185.
[59] P. Mendels, F. Bert, M.A. de Vries, A. Olariu, A. Harrison, F. Duc, J.-C. Trombe, J.S. Lord, A. Amato, C. Baines, Phys. Rev. Lett. 98 (2007) 077204.
[60] A. Zorko, S. Nellutla, J. van Tol, L.C. Brunel, F. Bert, F. Duc, J.-C. Trombe, M.A. de Vries, A. Harrison, P. Mendels, Phys. Rev. Lett. 101 (2008) 026405;
A. Zorko, et al., J. Phys. Conf. Ser. 145 (2009) 012014.
[61] S. El Shawish, O. Cépas, S. Miyashita, Phys. Rev. B 81 (2010) 224421.
[62] O. Cépas, C.M. Fong, P.W. Leung, C. Lhuillier, Phys. Rev. B 78 (2008) 140405.
[63] L. Messio, O. Cépas, C. Lhuillier, Phys. Rev. B 81 (2010) 064428.
[64] Y. Huh, L. Fritz, S. Sachdev, Phys. Rev. B 81 (2010) 144432.
[65] T.-H. Han, S. Chu, Y.S. Lee, Phys. Rev. Lett. 108 (2012) 157202.
[66] A. Zorko, et al., Phys. Rev. B 88 (2013) 144419.
[67] R.H. Colman, C. Ritter, A.S. Wills, Chem. Mater. 20 (2008) 6897–6899.
[68] R.H. Colman, A. Sinclair, A.S. Wills, Chem. Mater. 22 (2010) 5774–5779.
[69] B. Fåk, E. Kermarrec, L. Messio, B. Bernu, C. Lhuillier, F. Bert, P. Mendels, B. Koteswararao, F. Bouquet, J. Ollivier, A.D. Hillier, A. Amato, R.H. Colman, A.S. Wills, Phys. Rev. Lett. 109 (2012) 037208.
[70] A. Olariu, P. Mendels, F. Bert, F. Duc, J.-C. Trombe, M. de Vries, A. Harrison, Phys. Rev. Lett. 100 (2008) 087202.
[71] F. Bert, A. Olariu, A. Zorko, P. Mendels, J.-C. Trombe, F. Duc, M.A. de Vries, A. Harrisson, A.D. Hillier, J. Lord, A. Amato, C. Baines, J. Phys. 145 (2009) 012004.
[72] T. Imai, E.A. Nytko, B.M. Bartlett, M.P. Shores, D.G. Nocera, Phys. Rev. Lett. 100 (2008) 077203.
[73] O. Ofer, A. Keren, E.A. Nytko, M.P. Shores, B.M. Bartlett, D.G. Nocera, C. Baines, A. Amato, Phys. Rev. B 79 (2009) 134424.
[74] S. Miyahara, et al., Phys. Rev. B 75 (2007) 184402.

[75] M.A. de Vries, et al., Phys. Rev. Lett. 103 (2009) 237201.
[76] T.-H. Han, J.S. Helton, S. Chu, D.G. Nocera, J.A. Rodriguez-Rivera, C. Broholm, Y.S. Lee, Nature 492 (2012) 406.
[77] D. Wulferding, P. Lemmens, P. Scheib, J. Röder, P. Mendels, S. Chu, T. Han, Y.S. Lee, Phys. Rev. B 82 (2010) 144412.
[78] D.V. Pilon, C.H. Lui, T.-H. Han, D. Shrekenhamer, A.J. Frenzel, W.J. Padilla, Y.S. Lee, N. Gedik, Phys. Rev. Lett. 111 (2013) 127401.
[79] D.P. Kozlenko, A.F. Kusmartseva, E.V. Lukin, D.A. Keen, W.G. Marshall, M.A. de Vries, K.V. Kamenev, Phys. Rev. Lett. 108 (2012) 187207.
[80] M. Jeong, F. Bert, P. Mendels, F. Duc, J.C. Trombe, M.A. de Vries, A. Harrison, Phys. Rev. Lett. 107 (2011) 237201.
[81] I. Rousochatzakis, S.R. Manmana, A.M. Läuchli, B. Normand, F. Mila, Phys. Rev. B 79 (2009) 214415.
[82] M. Fu, T. Imai, T.-H. Han, Y.S. Lee, Science 350 (2015) 655.